



**Providing Choice & Value**  
Generic CT and MRI Contrast Agents

**FRESENIUS  
KABI**

**CONTACT REP**

**AJNR**

**Somatostatin Receptor–PET/CT/MRI of  
Head and Neck Neuroendocrine Tumors**

J.N. Rini, G. Keir, C. Caravella, A. Goenka and A.M.  
Franceschi

*AJNR Am J Neuroradiol* published online 13 July 2023  
<http://www.ajnr.org/content/early/2023/07/13/ajnr.A7934>

This information is current as  
of July 23, 2025.

# Somatostatin Receptor–PET/CT/MRI of Head and Neck Neuroendocrine Tumors

 J.N. Rini,  G. Keir,  C. Caravella,  A. Goenka, and  A.M. Franceschi



## ABSTRACT

**BACKGROUND AND PURPOSE:** Due to its high sensitivity, somatostatin receptor–PET may detect smaller lesions and more extensive disease than contrast-enhanced MR imaging, while the superior spatial resolution of MR imaging enables lesions to be accurately localized. We compared results of somatostatin receptor–PET/MRI with those of MR imaging alone and assessed the added value of vertex-to-thigh imaging for head and neck neuroendocrine tumors.

**MATERIALS AND METHODS:** Somatostatin receptor–PET/CT was acquired as limited brain or head and neck imaging, with optional vertex-to-thigh imaging, following administration of  $^{64}\text{Cu}/^{68}\text{Ga}$  DOTATATE. Somatostatin receptor–PET was fused with separately acquired contrast-enhanced MR imaging. DOTATATE activity was classified as comparable, more extensive, and/or showing additional lesions compared with MR imaging. Vertex-to-thigh findings were classified as positive or negative for metastatic disease or incidental.

**RESULTS:** Thirty patients (with 13 meningiomas, 11 paragangliomas, 1 metastatic papillary thyroid carcinoma, 1 middle ear neuroendocrine adenoma, 1 external auditory canal mass, 1 pituitary carcinoma, 1 olfactory neuroblastoma, 1 orbital mass) were imaged. Five had no evidence of somatostatin receptor–positive lesions and were excluded. In 11/25, somatostatin receptor–PET/MRI and MR imaging were comparable. In 7/25, somatostatin receptor–PET/MRI showed more extensive disease, while in 9/25, somatostatin receptor–PET/MRI identified additional lesions. On vertex-to-thigh imaging, 1 of 17 patients was positive for metastatic disease, 8 of 17 were negative, and 8 of 17 demonstrated incidental findings.

**CONCLUSIONS:** Somatostatin receptor–PET detected additional lesions and more extensive disease than contrast-enhanced MR imaging alone, while vertex-to-thigh imaging showed a low incidence of metastatic disease. Somatostatin receptor–PET/MRI enabled superior anatomic delineation of tumor burden, while any discrepancies were readily addressed. Somatostatin receptor–PET/MRI has the potential to play an important role in presurgical and radiation therapy planning of head and neck neuroendocrine tumors.

**ABBREVIATIONS:** FWHM = full width at half maximum; HNPGL = head and neck paraganglioma; max = maximum; NCCN = National Comprehensive Cancer Network; NET = neuroendocrine tumor; PitNET = pituitary neuroendocrine tumor; SSA = somatostatin analog; SSTR = somatostatin receptor; SUV = standard uptake value

Neuroendocrine tumors (NETs) are a heterogeneous group of neoplasms characterized by cell surface overexpression of somatostatin receptors (SSTRs). NETs occur throughout the body, most commonly in the gastrointestinal tract, pancreas, and lungs.<sup>1</sup> In the head and neck, the most common NETs are meningiomas and head and neck paragangliomas (HNPGLs).<sup>2–4</sup>

Less common entities include olfactory neuroblastoma, middle ear neuroendocrine tumors, medullary thyroid carcinoma, and pituitary lesions.<sup>5–7</sup>

SSTRs serve as the target for functional imaging of NETs using radiolabeled somatostatin analogues (SSAs). There are 5 main subtypes of SSTRs, with type 2 receptors most frequently overexpressed in NETs.<sup>8</sup> Functional imaging of NETs was originally performed with planar and SPECT imaging using  $^{111}\text{In}$  pentetate (OctreoScan; Mallinckrodt).<sup>9–11</sup> Since 2016, beginning with the FDA approval of  $^{68}\text{Ga}$  DOTATATE, the European Medicines Agency approval of  $^{68}\text{Ga}$  DOTATOC, and the subsequent FDA approval of  $^{64}\text{Cu}$  DOTATATE in 2020, functional imaging of NETs has transitioned to PET with SSAs,<sup>12</sup> a technique, collectively referred to as SSTR-PET. In 2017, the Society of Nuclear Medicine and Molecular Imaging recommended that SSTR-PET should replace  $^{111}\text{In}$  pentetate scintigraphy.<sup>13</sup>

Received March 20, 2023; accepted after revision June 14.

From the Nuclear Medicine Division (J.N.R., G.K., C.C.), Department of Radiology, and Department of Radiation Oncology (A.G.), Donald and Barbara Zucker School of Medicine at Hofstra/Northwell, Manhasset, New York; and Neuroradiology Division (A.M.F.), Department of Radiology, Donald and Barbara Zucker School of Medicine at Hofstra/Northwell, Lenox Hill Hospital, New York, New York.

Please address correspondence to Ana M. Franceschi, MD, PhD, Department of Radiology, Lenox Hill Hospital, 100 East 77th St, 3rd Floor, New York, NY 10075; e-mail: afranceschi@northwell.edu; @AFranceschi\_MDPhD

 Indicates article with online supplemental data.

<http://dx.doi.org/10.3174/ajnr.A7934>

## DOTATATE-PET/CT protocol parameters

Protocol	PET <sup>a</sup>		CT <sup>b</sup>	
	Bed Positions	Acquisition Time (Min/Bed)	mA	Pitch (mm/Rot)
Brain	1	10	95	1.375
Head/neck	3	5	Fixed mA	0.984
			50–440	
Vertex-to-thigh	7–8	5	Auto mA	0.984
			Noise index 18.0	
			30–440	
			Auto mA	
			Noise index 28.5	

**Note:**—Min indicates minute; Rot, rotation time.

<sup>a</sup> All 3D PET data were reconstructed using VUE Point FX (GE Healthcare) TOF and Sharp IR; <sup>64</sup>Cu-DOTATATE: 256 matrix, 3 iterations, 8 subsets, “standard” z-axis filter, and a Gaussian postfilter of 7.0-mm FWHM; <sup>68</sup>Ga DOTATATE: 192 matrix, 2 iterations, 24 subsets, standard z-axis filter, and a Gaussian postfilter of 6.4-mm FWHM.

<sup>b</sup> All helical CT configurations used 120 kV(peak), 3.75-mm section thickness, and a 0.8-second rotation.

Advantages of SSTR-PET, compared with scintigraphy, include improved sensitivity of lesion detection, lower radiation dose, and shorter and more convenient study duration.<sup>14,15</sup>

SSTR-PET is most frequently used to evaluate NETs that arise from gastroenteropancreatic sites. The Society of Nuclear Medicine and Molecular Imaging Appropriate Use Criteria for SSTR-PET focus on its role in well-differentiated gastroenteropancreatic NETs.<sup>13–15</sup> While the guidelines do not specifically address the role of SSTR-PET in head and neck tumors, they indicate that the technique will likely serve as a valuable tool for the assessment of many additional SSTR-positive diseases.<sup>13</sup> In fact, the current National Comprehensive Cancer Network (NCCN) Guidelines for Central Nervous System Cancers state that meningiomas exhibit high SSTR density, which allows the use of SSTR imaging to help delineate the extent of disease and to pathologically define an extra-axial lesion, as well as for distinguishing residual tumor from postoperative scarring in subtotally resected/recurrent tumors.<sup>16,17</sup> In addition, the NCCN guidelines suggest that SSTR-PET may also be indicated for medullary thyroid carcinoma, depending on the calcitonin/carcinoembryonic antigen doubling time.<sup>18</sup>

Due to its high sensitivity, SSTR-PET may detect smaller lesions and more extensive disease than contrast-enhanced MR imaging alone, while hybrid PET/MRI systems offer the added value of the superior spatial resolution of MR imaging, which enables a more accurate anatomic localization of lesions compared with PET or PET/CT.<sup>19</sup> Combined SSTR-PET/MRI is superior to either technique alone for oncologic imaging;<sup>20</sup> however, the availability of dedicated PET/MRI scanners in clinical practice remains limited. In the absence of simultaneous PET/MRI systems, SSTR-PET is routinely performed in the clinical setting as PET/CT from the vertex-to-thigh. Because distant metastases are uncommon with meningiomas and HNPGLs,<sup>21,22</sup> depending on the clinical indication, SSTR-PET imaging limited to the brain or head and neck may be sufficient for assessment of neuroendocrine tumors in the head and neck. The advantages of a limited SSTR-PET imaging include reduced imaging acquisition times, a shorter CT range, and a smaller display FOV, which is optimized for imaging of the brain and head and neck. Additionally, the anatomy included in both limited SSTR-PET

and separately acquired MR imaging is more successfully fused using neuroimaging postprocessing software compared with vertex-to-thigh PET, allowing SSTR-PET/MRI interpretation.

Therefore, we recently introduced a SSTR-PET/CT/MR imaging protocol for head and neck neuroendocrine tumor assessment. The protocol includes a limited SSTR-PET of the brain or head and neck, fusion with a separately acquired contrast-enhanced MR imaging using commercially available software, and an optional SSTR-PET/CT from vertex to thigh. The purpose of this study was to compare the results of limited SSTR-PET/MRI with those

of separately acquired MR imaging of the brain or head and neck and to assess the added value of vertex-to-thigh imaging.

## MATERIALS AND METHODS

Beginning in May 2022, before scheduling patients with known or suspected SSTR-positive head and neck tumors for SSTR-PET/CT, clinical notes and structural MR imaging/CT head and neck imaging were reviewed, and the study was protocolled by a nuclear medicine physician as a limited brain or head and neck study, with or without vertex-to-thigh imaging, based on lesion location and the request of the referring physician.

SSTR-PET/CT was acquired 50–60 minutes following IV administration of 148-MBq (4-mCi) <sup>64</sup>Cu DOTATATE or 185-MBq (5-mCi) <sup>68</sup>Ga DOTATATE using a Discovery 710HD (GE Healthcare) or a Biograph mCT 64 (Siemens) scanner. Imaging times for brain, head and neck, and vertex-to-thigh protocols were approximately 10, 15, and 40 minutes, respectively. Reconstruction parameters specific for <sup>64</sup>Cu DOTATATE included a 256 matrix, 3 iterations, 8 subsets, and a postfilter cutoff of 7.0-mm full width at half maximum (FWHM). Reconstruction parameters for <sup>68</sup>Ga DOTATATE included a 192 matrix, 2 iterations, 24 subsets, and a postfilter cutoff of 6.4-mm FWHM (Table). Limited SSTR-PET was corrected for attenuation using CT and was fused with separately acquired contrast-enhanced MR imaging of the brain or neck using MIMneuro software (Version 7.2.7; MIM software). Dedicated contrast-enhanced MR imaging of the brain and neck were interpreted by fellowship-trained neuroradiologists as part of routine clinical care. A fellowship-trained neuroradiologist with 10 years of experience in PET/MRI interpreted brain and head and neck SSTR-PET/MRI, while a nuclear medicine physician with 20 years of experience interpreted concurrently obtained vertex-to-thigh images.

Following institutional review board approval, the neuroradiologist classified DOTATATE activity as comparable, locally more extensive, and/or showing additional lesions, compared with separately acquired contrast-enhanced MR imaging of the brain or head and neck. The nuclear medicine physician classified vertex-to-thigh images, excluding the head and neck, as positive or negative for metastatic disease or as showing incidental findings.

## RESULTS

Thirty patients (25 females, 5 males; age range, 16–77 years; mean age, 55 years) with known or suspected SSTR-positive head and neck tumors were imaged with limited SSTR-PET/CT (limited brain [18/30, 60% patients], limited head and neck [12/30, 40% patients], and vertex-to-thigh [17/30, 57% patients]),

with either  $^{64}\text{Cu}$  DOTATATE (29 patients) or  $^{68}\text{Ga}$  DOTATATE (1 patient) (Online Supplemental Data). For 29/30 patients, limited SSTR-PET was fused with separately acquired contrast-enhanced MR imaging of the brain or MR imaging of the head and neck. For 1 patient with a cochlear implant, MR imaging was not performed.

Twenty-five patients had SSTR-positive lesions (including 12 meningiomas, 10 HBPGLs [3 glomus jugulare tumors, 2 glomus tympanicum tumors, 3 glomus jugulotympanicum tumors, 1 glomus vagale, 1 multiple cervical paraganglioma]; 1 had a suspected cervical paraganglioma on MR imaging of the neck with subsequent biopsy positive for metastatic papillary thyroid carcinoma, 1 had a pituitary carcinoma, and 1 had an olfactory neuroblastoma).

In 11/25 (44%) subjects, findings of SSTR-PET/MRI and contrast-enhanced MR imaging were comparable (Figs 1 and 2). In 7/25 (28%) patients, SSTR-PET/MRI showed locally more extensive disease than contrast-enhanced MR imaging alone (Figs 3 and 4). Of these 7 patients, 6 patients had meningiomas, typically imaged in the postoperative setting, with SSTR-PET/MRI detecting additional transosseous involvement (2 patients), recurrence at the craniotomy site (3 patients), and/or disease at the skull base (1 patient with prominent

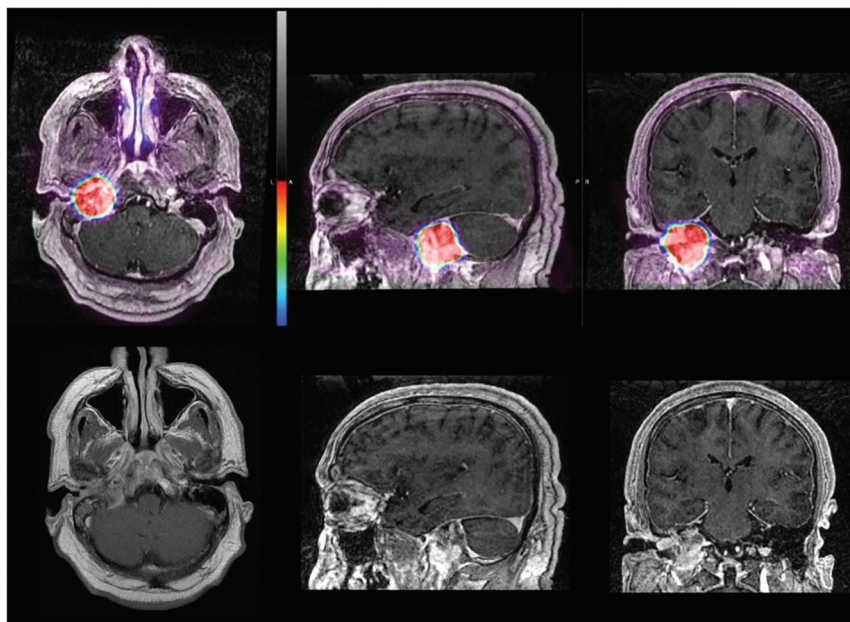


**FIG 1.** A 55-year-old man with a SSTR-avid mass centered in the right jugular fossa, which extends into the right middle ear cavity, measuring  $3.7 \times 3.6 \times 3.5$  cm, consistent with glomus jugulotympanicum paraganglioma. In this example, SSTR-PET/MRI findings are comparable with the extent of disease identified by contrast-enhanced MR imaging.

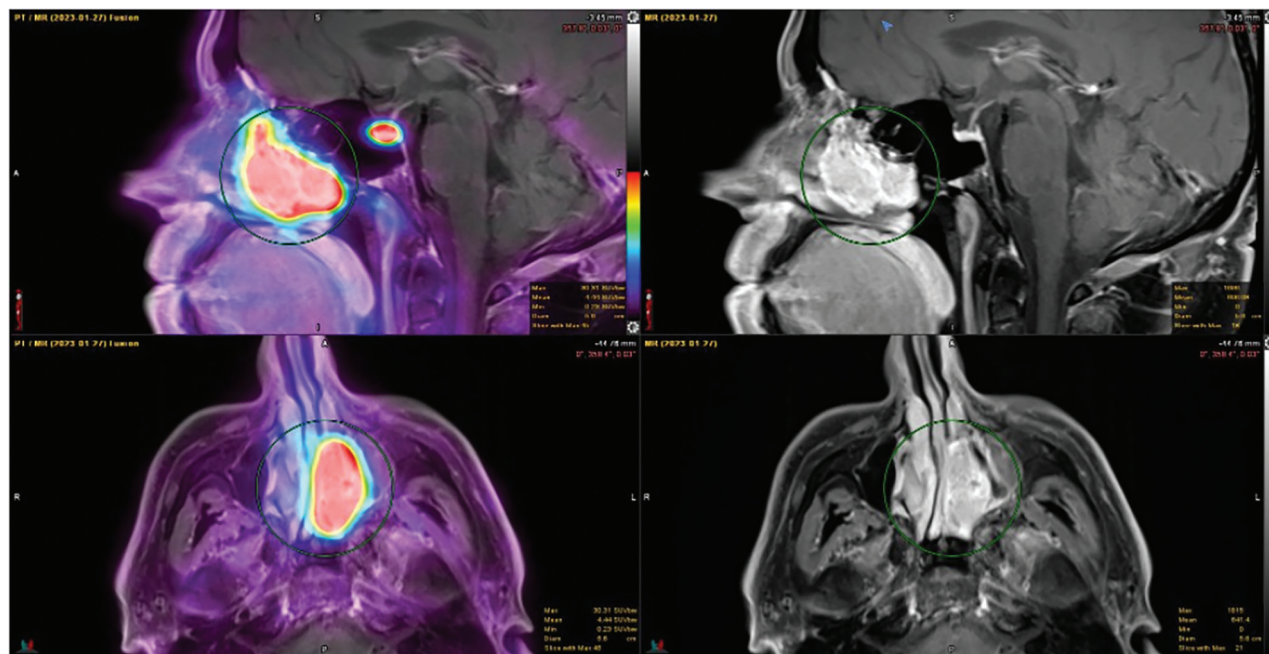


**FIG 2.** A 46-year-old man with a SSTR-avid homogeneously enhancing soft-tissue mass arising from the left nasal cavity, measuring  $4.0 \times 1.9 \times 4.1$  cm in anterior-posterior by transverse by craniocaudal dimensions, consistent with biopsy-proved olfactory neuroblastoma (esthesioneuroblastoma). There was no evidence of intracranial tumor extension. In this example, SSTR-PET/MRI findings are comparable with the extent of disease identified by contrast-enhanced MR imaging.



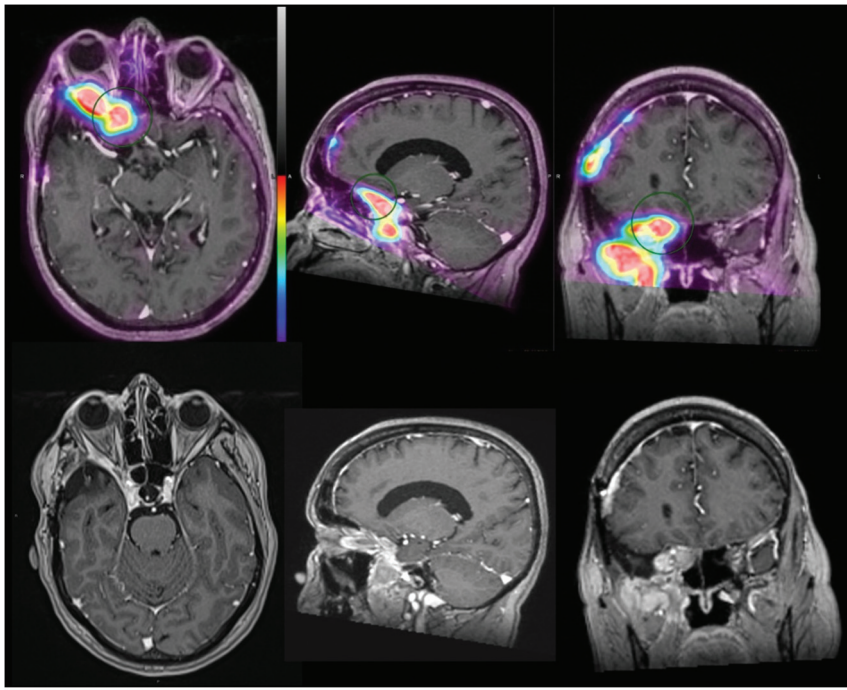


**FIG 3.** A 63-year-old woman post-right pterional craniotomy for meningioma resection with SSTR-avid recurrent meningioma arising from the right sphenoid wing and infiltrating the right orbital apex, right cavernous sinus, right sphenoid sinus, and right posterior ethmoid air cells and extending inferiorly along the right anterior temporal convexity and into the right masticator space. SSTR-positive recurrence is also noted at the right frontal craniotomy site. In this example, SSTR-PET/MRI findings were more extensive than on the basis of structural imaging because the extracranial tumor component was not identified on contrast-enhanced MR imaging.

extracranial tumor extension into the right masticator space), compared with contrast-enhanced MR imaging of the brain alone. One of the 7 patients had recurrent/residual pituitary carcinomas, which had progressed with the patient on somatostatin analog therapy. Meanwhile, in 9/25 (36%) subjects, SSTR-PET/MRI identified additional lesions (Fig 5). Most of these patients (5/9) had incidentally detected subcentimeter meningiomas, 1 patient had a parathyroid adenoma, and another had temporomandibular joint arthritis. Most interesting, in 2 patients, SSTR-PET/MRI detected additional glomus jugulare tumors, which were not identified by initial contrast-enhanced MR imaging. One of the patients presented with tongue weakness and fasciculations, with negative findings on MR imaging of the brain (retrospective review of the MR imaging revealed an enhancing lesion centered in the left jugular foramen and expanding the left hypoglossal canal). Given progressive symptoms, the patient underwent surgical exploration, but no lesion was identified. Subsequent SSTR-PET/MRI demonstrated a left glomus jugulare paraganglioma measuring  $1.4 \times 2.2 \times 1.7$  cm (maximum standard uptake value [SUVmax], 148.65). The patient was treated by stereotactic radiosurgery with curative intent. The second patient had multiple known cervical paragangliomas, previously assessed by contrast-enhanced MR imaging of the neck. In this case, SSTR-PET/MRI showed an additional, previously undetected right glomus jugulare tumor measuring  $0.5 \times 0.5$  cm (SUVmax, 29.63).

Five patients had no evidence of SSTR-positive lesions and were excluded from the final analysis. Three patients were imaged

with concern for tumor recurrence on contrast-enhanced MR imaging (meningioma, middle ear neuroendocrine adenoma, and carotid body tumor, respectively), but there was no evidence of SSTR-positive lesions to suggest residual or recurrent tumor. For 1 patient with an indeterminate mass in the left external auditory canal on MR imaging and CT of the temporal bones, SSTR-PET had negative findings, and findings favored cholesterol granuloma or cholesteatoma or, less likely, a low-grade non-SSTR-positive neoplasm. For 1 patient with an orbital mass concerning for optic nerve sheath meningioma versus orbital cavernous venous malformation (cavernous hemangioma), SSTR-PET was negative for the former, and findings favored orbital cavernous venous malformation (Fig 6).

For SSTR-PET/CT vertex-to-thigh imaging, 1 of 17 (6%) studies was positive for metastatic disease (an SSTR-positive lung nodule measuring 1.4 cm, SUVmax = 8.4, in a patient with biopsy confirmation of recurrent papillary thyroid carcinoma), and 8 of 17 (47%) studies were negative. On 8/17 (47%) SSTR-PET vertex-to-thigh studies, there were indeterminate/incidental findings, including nonavid subcentimeter lung nodules (3 subjects), ground glass lung opacity, adrenal adenoma, indeterminate gallbladder focus, indeterminate adrenal gland focus, a benign breast lesion (SSTR-avid breast lesion, benign on subsequent biopsy), probable benign cervical and axillary lymph nodes, leiomyomatous uterus, enlarged prostate gland with indeterminate focus, and nonspecific cutaneous foci (2 patients).

## DISCUSSION

Recent advances and the increased availability of hybrid PET/CT and PET/MRI systems are revolutionizing neuro-oncologic imaging. Specifically, the use of radiolabeled amino acid PET tracers, which bind to specific receptors on tumors, offers improved accuracy in defining the tumor versus background and guiding treatment strategies.<sup>23</sup> Furthermore, several  $^{68}\text{Ga}/^{64}\text{Cu}$ -labeled SSAs have recently entered clinical practice, allowing the detection of cell-surface expression of SSTRs, each varying in their short-chain peptide hormone analog and DOTA chelator.<sup>2,12</sup> DOTA-TATE is a radioconjugate that contains a SSA, TATE, radiolabeled with positron-emitting radionuclides,  $^{68}\text{Ga}$  or  $^{64}\text{Cu}$ , via a chelating agent, DOTA. SSTR-targeted PET imaging has several advantages over scintigraphy, including improved spatial resolution and accuracy, decreased radiation dose and cost, and increased patient convenience due to the relatively short radiopharmaceutical half-life.<sup>2</sup> Because SSTR-PET identifies more lesions than structural imaging alone,<sup>4</sup> it should be considered an integral

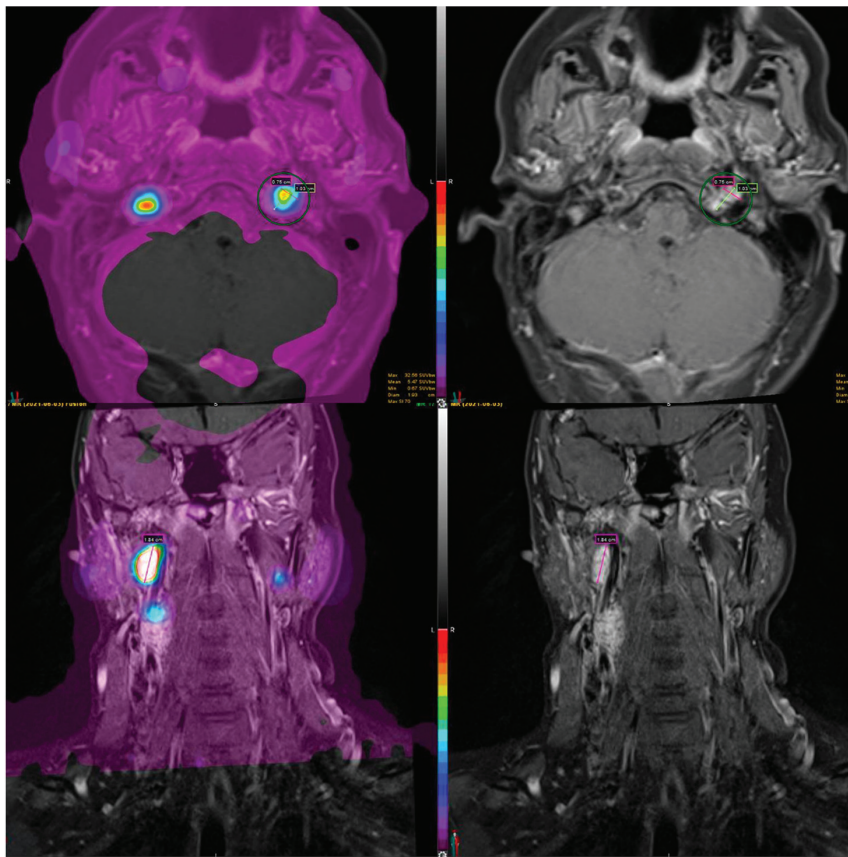


**FIG 4.** A 31-year-old woman with a vividly enhancing submandibular mass positive for neuroendocrine markers. The patient had SSTR-avid carotid body tumors, a glomus vagale tumor, and glomus jugulare tumors bilaterally. In this example, SSTR-PET/MRI findings were more extensive than on the basis of structural imaging because the right glomus jugulare tumor was not identified on contrast-enhanced MR imaging.

element of clinical management for suspected neuroendocrine tumors in the head and neck. Hybrid PET/MRI allows the systematic addition of high-resolution MR imaging to PET, thereby providing precise and consistent anatomic information, which helps to overcome difficulties in localization inherent to PET and may exclude or identify the presence of multiple pathologies.<sup>19</sup> SSTRs are overexpressed in many tumors of the head and neck, including meningiomas, HNPGLs, middle ear NETs, olfactory neuroblastomas, medullary thyroid carcinoma, and pituitary lesions such as pituitary neuroendocrine tumors (PitNETs, formerly known as pituitary adenomas)<sup>24</sup> and pituitary carcinomas.<sup>3-7</sup>

Meningiomas are the most common primary intracranial tumors. Approximately 50% of patients may undergo a subtotal tumor resection, which is associated with lower overall survival and lower progression-free survival.<sup>21</sup> Contrast-enhanced MR imaging of the brain is the current standard of care for the diagnosis and treatment planning of meningiomas; however, it can be limited in the setting of postsurgical or postradiation treatment changes. In addition, MR imaging may be limited if lesions are infiltrative, transosseous, or in the region of the skull base and cavernous sinus.<sup>3</sup> SSTR-PET/MRI has demonstrated promise in the assessment of resected and irradiated meningiomas, with improved sensitivity and disease-extent evaluation, particularly in

cases in which MR imaging findings are equivocal.<sup>3,26</sup> In our series, SSTR-PET/MRI identified additional meningiomas in 4 of 13 (31%) patients imaged for meningioma follow-up. Additionally, 2 new meningiomas were identified by SSTR-PET/MRI in a patient who was imaged for an unrelated head and neck lesion (glomus tympanicum). In 6 of 13 (46%) patients with meningiomas, a greater extent of disease was identified by SSTR-PET/MRI compared with contrast-enhanced MR imaging alone, with SSTR-PET/MRI typically detecting transosseous involvement, recurrent/residual tumor at the craniotomy site, and disease at the skull base. In fact, in only 3 of the 13 patients with meningiomas (23%), findings were the same on SSTR-PET/MRI compared with structural imaging. The results of SSTR-PET/MRI helped guide the planning of stereotactic radiation therapy for patients with meningiomas at our institution, as has been described in the literature.<sup>25-29</sup> In fact, when incorporating SSTR-PET/MRI into radiation treatment-planning of intermediate-risk meningiomas, Mahase et al<sup>28</sup> demonstrated a 50% reduction in the dose to several critical structures, with no local recurrences at 6 months. Kim et al<sup>25</sup> found a sensitivity as high as 86.1% and a specificity as high as 97.6% when

using different diagnostic SUV thresholds for meningioma diagnosis. An important caveat is that SSTR-negative meningiomas are known to occur; however, they are exceedingly rare.<sup>30</sup>

The diagnosis of neuroendocrine tumors, including HNPGLs, is challenging because symptoms are highly variable and the tumors are often small. In fact, there is typically a delay of 5–7 years from the first symptoms to diagnosis in these patients.<sup>22</sup> SSTR expression can be seen physiologically in a number of organs, including the spleen, adrenal glands, kidneys, pituitary gland, liver, thyroid, and salivary glands.<sup>31</sup> Because HNPGLs occur in locations that typically do not demonstrate SSTRs, SSTR-PET is optimally positioned to help delineate known lesions and assess additional paragangliomas not identified by structural imaging.<sup>2,4,31</sup> Janssen et al<sup>4</sup> found that <sup>68</sup>Ga DOTATATE PET identified more paragangliomas than other imaging modalities, including [<sup>18</sup>F] FDOPA, [<sup>18</sup>F] FDG, and [<sup>18</sup>F] FDOPA PET/CT, and contrast-enhanced CT or MR imaging. The identification of multiple neuroendocrine tumors can have important implications for genetic testing and hereditary information that can impact not only the patient but also family members, who may undergo screening as a result. In patients with an *SDHx* mutation predisposed to multiple hereditary paragangliomas and pheochromocytomas, guidelines recommend head and neck MRA and SSTR



imaging, in addition to CT of the chest, abdomen, and pelvis.<sup>32,33</sup> In our study, SSTR-PET/MRI found additional paragangliomas in 2 of 11 subjects with HNPGL (18%), which were not suspected by contrast-enhanced MR imaging of the brain or neck. One of these

patients presented with tongue weakness and fasciculations, with 2 MR imaging studies with negative findings and negative surgical exploration of the left skull base, while the other patient had multiple known cervical paragangliomas, with an additional glomus jugulare detected by SSTR-PET/MRI. Furthermore, in 2 patients imaged for HNPGL assessment, SSTR-PET/MRI identified additional lesions, including 2 meningiomas, a PitNET, and a parathyroid adenoma.

Olfactory neuroblastoma (esthesioneuroblastoma) is a rare sinonasal neuroendocrine tumor thought to originate from the stem cells of the olfactory epithelium.<sup>5</sup> Although olfactory neuroblastomas have a relatively favorable prognosis, no standardized treatment guidelines have been established. One complicating factor has been their propensity for locoregional recurrence.<sup>34</sup> [<sup>18</sup>F] FDG-PET is frequently used for tumor staging in patients with advanced disease and evaluating treatment response.<sup>35</sup> However, olfactory neuroblastomas also demonstrate high SSTR expression, and the application of SSTR-targeted imaging with histologic correlation was initially demonstrated by Rostomily et al,<sup>36</sup> using <sup>111</sup>In-pentetreotide scintigraphy. Since then, molecular imaging of olfactory neuroblastomas has transitioned to

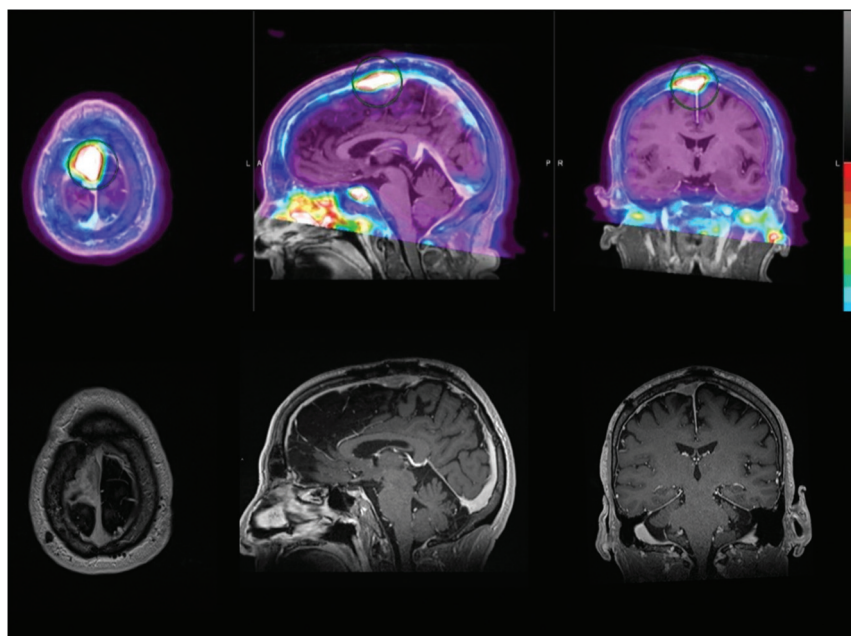


**FIG 5.** A 69-year-old woman with a SSTR-avid recurrent meningioma in the right frontal parasagittal region and associated invasion of the calvaria and superior sagittal sinus. Incidentally noted is SSTR-positivity in the left temporomandibular joint with prominent articular/periarticular enhancement, suggestive of inflammatory/infectious arthritis. In this example, SSTR-PET/MRI findings are more extensive than on the basis of structural imaging because calvarial invasion was not identified by contrast-enhanced MR imaging of the brain.

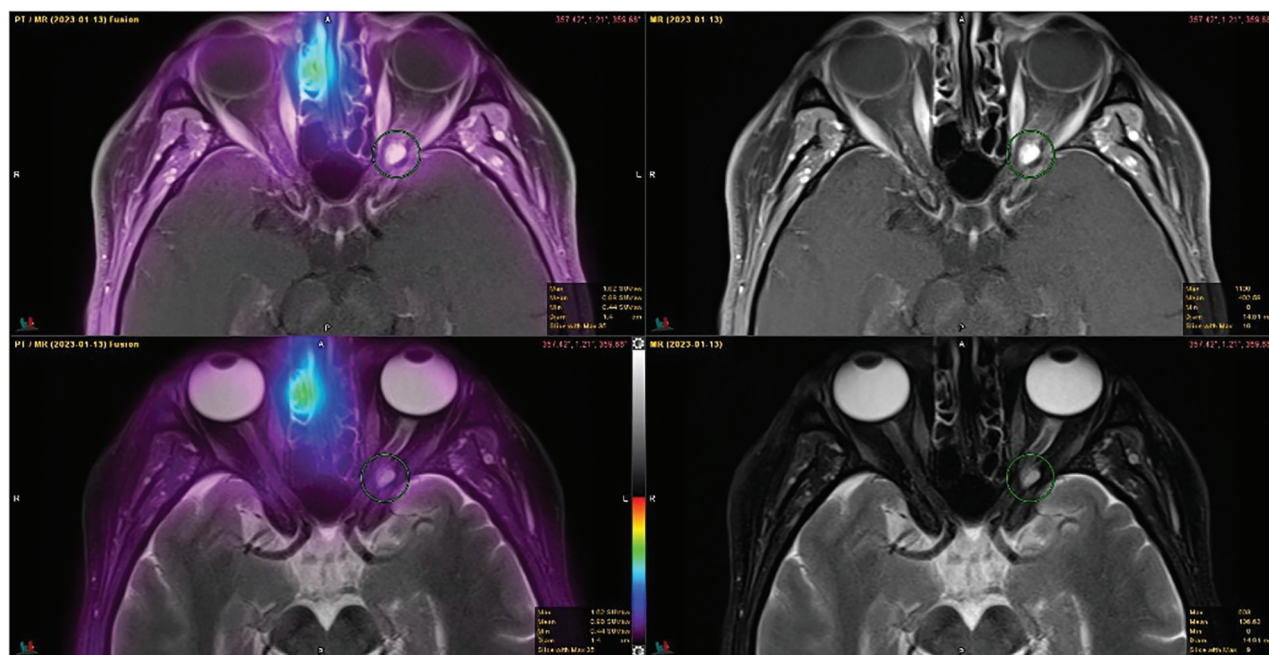


**FIG 6.** A 52-year-old woman presenting with a visual field disturbance and contrast-enhanced MR imaging demonstrating a left orbital mass concerning for orbital nerve sheath meningioma versus orbital cavernous venous malformation (cavernous hemangioma). Findings of SSTR-PET were negative and represent an orbital cavernous venous malformation. The patient was subsequently referred for surgical management.

PET with  $^{68}\text{Ga}$ -/ $^{64}\text{Cu}$ -labeled SSAs. In 1 cohort, Roytman et al<sup>5</sup> found that DOTATATE-PET/MRI demonstrated utility in evaluating treatment response, identifying metastases and soft-tissue metastatic burden, and distinguishing inflammatory from metastatic adenopathy. The distinction between inflammatory and metastatic adenopathy was particularly useful compared with metabolic [ $^{18}\text{F}$ ] FDG-PET. An important caveat is that low-level SSTR expression may be seen with infection or inflammation, including in the resection cavity in the immediate postoperative setting. In our single case of olfactory neuroblastoma, SSTR-PET/MRI found the same extent of disease as contrast-enhanced MR imaging had; however, it helped to confirm the absence of locoregional metastases, which are found in 10%–44% of patients at the time of diagnosis.<sup>33</sup>

Finally, PitNETs are the third most common intracranial neoplasm. Approximately 30% are nonfunctional adenomas, lacking early clinical and biochemical signs.<sup>37</sup> Thus, they often present due to symptoms of mass effect once they reach >1 cm (macroadenomas). These lesions are difficult to treat because surgical resection may be incomplete, especially when the cavernous sinus is involved, and adjuvant radiation therapy may be associated with hypopituitarism and neurocognitive impairment.<sup>37</sup> Immunohistochemical studies have demonstrated that SSTRs are expressed in a varying proportion of nonfunctional adenomas.<sup>38–40</sup> In a study of 37 patients with nonfunctional adenomas diagnosed in the context of a clinical trial for lanreotide (SSA) therapy, 34/37 (92%) were positive by  $^{68}\text{Ga}$  DOTATATE PET using an SUVmean of >2 cutoff, which may assist in predicting tumor response to SSTR type 2 preferential SSA therapy.<sup>6</sup> Meanwhile, pituitary carcinomas are rare neoplasms and are associated with a poor prognosis. A case report by Xiao et al<sup>41</sup> suggested that  $^{68}\text{Ga}$  DOTATATE-PET was superior to [ $^{18}\text{F}$ ] FDG-PET for lesion assessment, though the affinity of  $^{68}\text{Ga}$  DOTATATE compared with [ $^{18}\text{F}$ ] FDG varies depending on the aggressiveness of the tumor.<sup>7</sup> In addition,  $^{68}\text{Ga}$  DOTATATE-PET has demonstrated promise in identifying patients with pituitary carcinomas who are candidates for  $^{177}\text{Lu}$  DOTATATE (LUTATHERA; Advanced Accelerator Applications) peptide receptor radionuclide therapy and monitoring treatment response.<sup>42</sup> In our case of pituitary carcinoma, the patient was treated with a SSA (lanreotide) following resection and prior radiation and systemic chemotherapy. SSTR-PET/MRI identified a greater extent of disease and confirmed progression of disease while the patient was on lanreotide, compared with contrast-enhanced MR imaging alone.

## CONCLUSIONS

In our series of head and neck neuroendocrine tumors, SSTR-PET/MRI detected additional lesions and more extensive disease compared with contrast-enhanced MR imaging. While SSTR-PET/MRI is superior to either technique alone,<sup>19</sup> the availability of simultaneous PET/MRI scanners in clinical practice remains limited. In the absence of a dedicated hybrid PET/MRI system, limited SSTR-PET may be fused with separately acquired contrast-enhanced MR imaging of the brain or head and neck using commercially available software, as presented here, thereby enabling PET/MRI assessment in a real-world clinic setting. In addition, vertex-to-thigh imaging showed a low incidence of

metastatic disease, raising the possibility that limited imaging of the head and neck may be sufficient in this patient population. However, in patients with syndromes and/or genetic disorders, a limited head and neck protocol may miss other occult lesions throughout the body. Therefore, the choice of SSTR-PET imaging protocol ultimately depends on a discussion with the referring clinician and careful review of clinical history on a case-by-case basis. In conclusion, SSTR-PET/MRI has the potential to play an important role in presurgical and radiation therapy planning of head and neck neuroendocrine tumors, as well as for monitoring treatment response and evaluating tumor recurrence in these patients.

**Disclosure forms** provided by the authors are available with the full text and PDF of this article at [www.ajnr.org](http://www.ajnr.org).

## REFERENCES

- Schimmack S, Svejda B, Lawrence B, et al. **The diversity and commonalities of gastroenteropancreatic neuroendocrine tumors.** *Langenbecks Arch Surg* 2011;396:273–98 [CrossRef Medline](#)
- Ivanidze J, Roytman M, Sasson A, et al. **Molecular imaging and therapy of somatostatin receptor positive tumors.** *Clin Imaging* 2019;56:146–54 [CrossRef Medline](#)
- Ivanidze J, Roytman M, Lin E, et al. **Gallium-68 DOTATATE PET in the evaluation of intracranial meningiomas.** *J Neuroimaging* 2019;29:650–56 [CrossRef Medline](#)
- Janssen I, Chen CC, Taieb D, et al.  **$^{68}\text{Ga}$ -DOTATATE PET/CT in the localization of head and neck paragangliomas compared with other functional imaging modalities and CT/MRI.** *J Nucl Med* 2016;57:186–91 [CrossRef Medline](#)
- Roytman M, Tassler AB, Kacker A, et al. **[ $^{68}\text{Ga}$ ]-DOTATATE PET/CT and PET/MRI in the diagnosis and management of esthesioneuroblastoma: illustrative cases.** *J Neurosurg Case Lessons* 2021;1: CASE2058 [CrossRef Medline](#)
- Boertien TM, Booi J, Majoie CB, et al.  **$^{68}\text{Ga}$ -DOTATATE PET imaging in clinically non-functioning pituitary macroadenomas.** *Eur J Hybrid Imaging* 2020;4:4 [CrossRef Medline](#)
- Garnes HM, Carvalho JB, Reis F, et al. **Pituitary carcinoma: a case report and discussion of potential value of combined use of  $^{68}\text{Ga}$ -DOTATATE and  $^{18}\text{F}$ -FDG PET/CT scan to better choose therapy.** *Surg Neurol Int* 2017;8:162 [CrossRef Medline](#)
- John M, Meyerhof W, Richter D, et al. **Positive somatostatin receptor scintigraphy correlates with the presence of somatostatin receptor subtype 2.** *Gut* 1996;38:33–39 [CrossRef Medline](#)
- Krenning EP, Kwekkeboom DJ, Bakker WH, et al. **Somatostatin receptor scintigraphy with [ $^{111}\text{In}$ -DTPA-D-Phe1]- and [ $^{123}\text{I}$ -Tyr3]-octreotide: the Rotterdam experience with more than 1000 patients.** *Eur J Nucl Med* 1993;20:716–31 [CrossRef Medline](#)
- Bombardieri E, Ambrosini V, Aktolun C, et al; Oncology Committee of the EANM.  **$^{111}\text{In}$ -pentetreotide scintigraphy: procedure guidelines for tumour imaging.** *Eur J Nucl Med Mol Imaging* 2010;37:1441–48 [CrossRef Medline](#)
- Lamberts SW, Bakker WH, Reubi JC, et al. **Somatostatin-receptor imaging in the localization of endocrine tumors.** *N Engl J Med* 1990;323:1246–49 [CrossRef Medline](#)
- Johnbeck CB, Knigge U, Loft A, et al. **Head-to-head comparison of  $^{64}\text{Cu}$ -DOTATATE and  $^{68}\text{Ga}$ -DOTATOC PET/CT: a prospective study of 59 patients with neuroendocrine tumors.** *J Nucl Med* 2017;58:451–57 [CrossRef Medline](#)
- Hope TA, Bergsland EK, Bozkurt MF, et al. **Appropriate use criteria for somatostatin receptor PET imaging in neuroendocrine tumors.** *J Nucl Med* 2018;59:66–74 [CrossRef Medline](#)
- Hope TA. **Updates to the appropriate-use criteria for somatostatin receptor PET.** *J Nucl Med* 2020;61:1764 [CrossRef Medline](#)



15. Hope TA, Allen-Auerbach M, Bodei L, et al. SNMMI procedure standard/EANM practice guideline for SSTR-PET: imaging neuroendocrine tumors. *J Nucl Med* 2023;64:204–10 [CrossRef Medline](#)
16. Horbinski C, Nabors LB, Portnow J, et al. NCCN Guidelines Insights: Central Nervous System Cancers, Version 2.2022. *Natl Compr Canc Netw* 2023;21:12–20 [CrossRef Medline](#)
17. Nabors LB, Portnow J, Ahluwalia M, et al. Central Nervous System Cancers, Version 3.2020, NCCN Clinical Practice Guidelines in Oncology. *J Natl Compr Canc Netw* 2020;18:1537–70 [CrossRef Medline](#)
18. Haddad RI, Bischoff L, Ball D, et al. Thyroid Carcinoma, Version 2.2022, NCCN Clinical Practice Guidelines in Oncology. *J Natl Compr Canc Netw* 2022;20:925–51 [CrossRef Medline](#)
19. Catana C. Principles of simultaneous PET/MR imaging. *Magn Reson Imaging Clin N Am* 2017;25:231–43 [CrossRef Medline](#)
20. Mayerhoefer ME, Prosch H, Beer L, et al. PET/MRI versus PET/CT in oncology: a prospective single-center study of 330 examinations focusing on implications for patient management and cost considerations. *Eur J Nucl Med Mol Imaging* 2020;47:51–60 [CrossRef Medline](#)
21. Rogers L, Barani I, Chamberlain M, et al. Meningiomas: knowledge base, treatment outcomes, and uncertainties: a RANO review. *J Neurosurg* 2015;122:4–23 [CrossRef Medline](#)
22. Yao JC, Hassan M, Phan A, et al. One hundred years after “carcinoid”: epidemiology of and prognostic factors for neuroendocrine tumors in 35,825 cases in the United States. *J Clin Oncol* 2008;26:3063–72 [CrossRef Medline](#)
23. Pimlott SL, Sutherland A. Molecular tracers for the PET and SPECT imaging of disease. *Chem Soc Rev* 2011;40:149–62 [CrossRef Medline](#)
24. Trouillas J, Jaffrain-Rea ML, Vasiljevic A, et al. How to classify the pituitary neuroendocrine tumors (PitNET)s in 2020. *Cancers (Basel)* 2020;12:514 [CrossRef Medline](#)
25. Kim SH, Roytman M, Madera G, et al. Evaluating diagnostic accuracy and determining optimal diagnostic thresholds of different approaches to [68Ga]-DOTATATE PET/MRI analysis in patients with meningioma. *Sci Rep* 2022;12:9256 [CrossRef Medline](#)
26. Nyuyki F, Plotkin M, Graf R, et al. Potential impact of 68Ga-DOTATOC PET/CT on stereotactic radiotherapy planning of meningiomas. *Eur J Nucl Med Mol Imaging* 2010;37:310–18 [CrossRef Medline](#)
27. Prasad RN, Perlow HK, Bovi J, et al. 68Ga-DOTATATE PET: the future of meningioma treatment. *Int J Radiat Oncol Biol Phys* 2022;113:868–71 [CrossRef Medline](#)
28. Mahase SS, Roth O'Brien DA, No D, et al. [68Ga]-DOTATATE PET/MRI as an adjunct imaging modality for radiation treatment planning of meningiomas. *Neurooncol Adv* 2021;3:vdab012 [CrossRef Medline](#)
29. Hintz EB, Park DJ, Ma D, et al. Using 68Ga-DOTATATE PET for postoperative radiosurgery and radiotherapy planning in patients with meningioma: a case series. *Neurosurgery* 2023;93:95–101 [CrossRef Medline](#)
30. Roytman M, Pisapia DJ, Liechty B, et al. Somatostatin receptor-2 negative meningioma: pathologic correlation and imaging implications. *Clin Imaging* 2020;66:18–22 [CrossRef Medline](#)
31. Shastri M, Kayani I, Wild D, et al. Distribution pattern of 68Ga-DOTATATE in disease-free patients. *Nucl Med Commun* 2010;31:1025–32 [CrossRef Medline](#)
32. Gimenez-Roqueplo AP, Caumont-Prim A, Houzard C, et al. Imaging work-up for screening of paraganglioma and pheochromocytoma in SDHx mutation carriers: a multicenter prospective study from the PGL EVA Investigators. *J Clin Endocrinol Metab* 2013;98:E162–73 [CrossRef Medline](#)
33. Ikram A, Paraganglioma RA. *StatPearls*. StatPearls Publishing, 2022. <https://www.ncbi.nlm.nih.gov/books/NBK549834/>. Accessed May 22, 2023
34. Zollinger LV, Wiggins RH, Cornelius RS, et al. Retropharyngeal lymph node metastasis from esthesioneuroblastoma: a review of the therapeutic and prognostic implications. *AJNR Am J Neuroradiol* 2008;29:1561–63 [CrossRef Medline](#)
35. Dublin AB, Bobinski M. Imaging characteristics of olfactory neuroblastoma (esthesioneuroblastoma). *J Neurol Surg B Skull Base* 2016;77:1–5 [CrossRef Medline](#)
36. Rostomily RC, Elias M, Deng M, et al. Clinical utility of somatostatin receptor scintigraphic imaging (octreoscan) in esthesioneuroblastoma: a case study and survey of somatostatin receptor subtype expression. *Head Neck* 2006;28:305–12 [CrossRef Medline](#)
37. Even-Zohar N, Greenman Y. Management of NFAs: medical treatment. *Pituitary* 2018;21:168–75 [CrossRef Medline](#)
38. Fusco A, Giampietro A, Bianchi A, et al. Treatment with octreotide LAR in clinically non-functioning pituitary adenoma: results from a case-control study. *Pituitary* 2012;15:571–78 [CrossRef Medline](#)
39. Gabalec F, Drastikova M, Cesak T, et al. Dopamine 2 and somatostatin 1-5 receptors coexpression in clinically non-functioning pituitary adenomas. *Physiol Res* 2015;64:369–77 [CrossRef Medline](#)
40. Ramirez C, Cheng S, Vargas G, et al. Expression of Ki-67, PTTG1, FGFR4, and SSTR 2, 3, and 5 in nonfunctioning pituitary adenomas: a high throughput TMA, immunohistochemical study. *J Clin Endocrinol Metab* 2012;97:1745–51 [CrossRef Medline](#)
41. Xiao J, Zhu Z, Zhong D, et al. Improvement in diagnosis of metastatic pituitary carcinoma by 68Ga DOTATATE PET/CT. *Clin Nucl Med* 2015;40:129–31 [CrossRef Medline](#)
42. Novruzov F, Aliyev JA, Jaunmuktane Z, et al. The use of 68Ga DOTATATE PET/CT for diagnostic assessment and monitoring of 177Lu DOTATATE therapy in pituitary carcinoma. *Clin Nucl Med* 2015;40:47–49 [CrossRef Medline](#)